A new type of vacancy-induced localized states in multilayer graphene

Eduardo V. Castro,[1,2] María P. López-Sancho,[1] María A. H. Vozmediano[1]

[1]*Instituto de Ciencia de Materiales de Madrid, CSIC, Cantoblanco, E-28049 Madrid, Spain and*
[2]*Centro de Física do Porto, Rua do Campo Alegre 687, P-4169-007 Porto, Portugal*

We demonstrate the existence of a new type of zero energy state associated to vacancies in multilayer graphene that has a finite amplitude over the layer with a vacancy and adjacent layers, and the peculiarity of being quasi-localized in the former and totally delocalized in the adjacent ones. In a bilayer, when a gap is induced in the system by applying a perpendicular electric field, these states become truly localized with a normalizable wavefunction. A transition from a localized to an extended state can be tuned by the external gate for experimentally accessible values of parameters.

Graphene is a one atom thick layer of carbon atoms ordered in a honeycomb lattice. The enormous interest risen since its discovery [1] is driven equally by potential technological applications [2] and unconventional low-energy behavior (massless Dirac quasi-particles) [3]. Together with single layer graphene (SLG), bilayer graphene (BLG) and multilayer graphene (MLG) structures were also synthesized. The BLG structure being unique as a low energy effective model [4], rises better technological expectations due to the possibility to open and tune a gap in the spectrum by electric field effect [5–7]. A proper understanding of the effect of disorder is crucial for technology relevant applications. Annealing and removing the substrate has recently lead to an increase in mobility by one order of magnitude in SLG [8, 9]. Intrinsic defects, such as vacancies or topological lattice defects are not easy to get rid of and further investigation on their role is mandatory. Vacancies are lately been recognized as one of the most important scattering centers in SLG and BLG [10, 11] and the zero modes induced by this type of defects can greatly affect the transport properties of the samples as well as the possible electronic instabilities near the neutrality point.

In the present manuscript we address the character of vacancy-induced electronic states in BLG, with extension to the case. We begin by summarizing the main findings of this work. (i) For the minimal model we construct an analytic solution on the lattice for the zero modes associated to the two different types of vacancies in BLG – located at $A1/B2$ or $B1/A2$ [see Fig. 1(a)]. We demonstrate that a new type of state different from these found in SLG and in other layered systems exists in BLG. The peculiarity consists in having a finite amplitude over the two layers and, more exotic, the wave function is quasi-localized in one layer and totally delocalized in the other. We also prove that these states survive in the continuum limit. The states associated to the $A1/B2$-vacancies are quasi-localized decaying as $1/r$ at large distances, similar to these of SLG, while those corresponding to a $B1/A2$-vacancy are delocalized. The delocalization is due to the spread of the wave function in the opposite layer where the vacancy resides. This solution is directly applica-
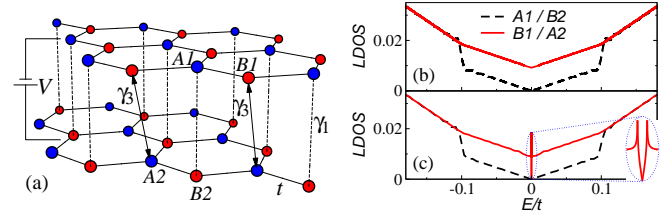

Figure 1: (color online). (a) Bilayer lattice structure and main tight-binding parameters. (b)-(c) LDOS for $\gamma_3 = 0$ and $\gamma_3 = 0.1t$, respectively.

ble to MLG and graphite. (ii) We demonstrate that these localization properties survive in the presence of non-minimal coupling γ_3 by means of a numerical analysis including the study of the participation ratios. (iii) We study the behavior of these states in the presence of a gap and find that these associated to the $B1/A2$-vacancy become truly localized states leaving inside the gap while the $A1/B2$-vacancy (monolayer type) become delocalized. The truly localized states are located symmetrically around the middle of the gap – depending on the layer they belong to.

Model.—The tight-binding minimal model for the $\pi-$electrons in AB-stacked BLG is schematically shown in Fig. 1(a). We will use the parameters $t \approx 3$ eV and $\gamma_1 \approx t/10$ [3]. It has two parabolic bands that touch at two degenerate Fermi points with a constant density of states (DOS) at the Fermi points. For the present study of zero modes it will also be of interest to consider the interlayer hopping $\gamma_3 \approx \gamma_1/3$ that linearizes the bands around the Fermi points and induces a vanishing DOS at zero energy. Figure 1 shows the local DOS (LDOS) for $\gamma_3 = 0$ (b) and $\gamma_3 \neq 0$ (c). The presence of a finite gap induced through a perpendicular electric field $E_z = V/(ed)$, where $d \approx 0.34$ nm is the interlayer distance, is included by adding an on-site energy term: $-V/2$ at layer 1 and $V/2$ at layer 2. Within the present model vacancies correspond to the elimination of lattice sites. We do not include any reconstruction of the remaining structure. Even though some reconstruction might be present in real systems, the zero-energy modes we are interested in
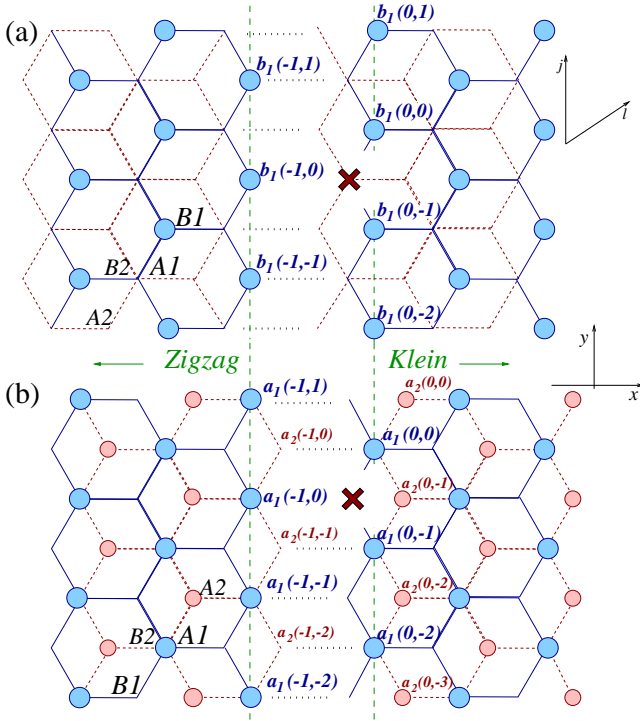
Figure 2: (color online). Schematics for constructing a vacancy-induced zero-energy solution in bilayer graphene (see text). Circles indicate sites where the localized states have a finite amplitude. (a) $A1/B2$ vacancy. (b) $B1/A2$ vacancy.

here seem to be rather insensitive to it [12].

Analytic construction of the vacancy states.—A vacancy in the honeycomb lattice gives rise to a quasi-localized state [13] whose wave function can be written as

$$\Psi(x,y) \approx \frac{e^{i\mathbf{K}.\mathbf{r}}}{x+iy} + \frac{e^{i\mathbf{K'}.\mathbf{r}}}{x-iy}, \qquad (1)$$

where $\mathbf{K}$ and $\mathbf{K'}$ are the reciprocal space vectors of the two inequivalent corners of the first Brillouin zone, and (x,y) are distances in a reference frame centered at the vacancy position. We will construct an analytic solution for vacancy-states in BLG within the minimal model following the analysis done for SLG in [13]. The wave function is obtained by matching surface state solutions at zigzag edges with those localized at Klein edges for a suitable boundary condition. The schematics used in this construction is shown in Fig. 2. The amplitude of the zero-mode wavefunction is denoted $c_i(l,j)$, with $c=a,b$ and $i=1,2$ for sites in sublattice A, B and layer $1,2$ of the unit cell located at (l,j). By cutting the system into *left* and *right* regions, defined with respect to the vacancy position, we see that in order to have a solution that decays away from the vacancy we need a zigzag-edge surface state to the left and a Klein-edge surface state to the right. The existence of surface states localized at zigzag edges in BLG has been proven in Ref. [14].

There are two linearly independent solutions, one living in a single layer (monolayer type) and the other having a finite amplitude over the two layers (bilayer type). Only sites belonging to the sublattice containing the zigzag edge have a finite amplitude. In an analogous way, one can show that surface states localized at Klein edges in BLG exist as well [15]. Again, two linearly independent solutions show up (monolayer and bilayer types).

Consider a vacancy at $A1/B2$ sites, as sketched in Fig 2(a). The zigzag- and Klein-edge surface states to be used have to have a finite amplitude, respectively, on the first zigzag column to the left and on the first beard column to the right of the vacancy. This is imposed by the matching (boundary) condition, which reads

$$b_1(-1, j) + b_1(0, j) + b_1(0, j-1) = 0 \qquad (2)$$

for all j's except at the vacancy, and involves sites of the two mentioned columns. The zigzag- and Klein-edge states with amplitudes starting at these columns are those of the monolayer type, i.e. with weight only on one layer:

$$b_1(l < 0, j) = \sum_{k_m} b_1(-1, k_m) D_{k_m}^{-(l+1)} e^{ik_m(\frac{l+1}{2}+j)}, \quad (3)$$

$$b_1(l \geq 0, j) = \sum_{k_{m'}} b_1(0, k_{m'}) D_{k_{m'}}^{-l} e^{ik_{m'}(\frac{l}{2}+j)}, \qquad (4)$$

where $D_k = -2\cos(k/2)$, and the sums go over $2\pi/3 \leq k_m \leq 4\pi/3$ in Eq. (3) and $0 \leq k_{m'} \leq 2\pi/3$ and $4\pi/3 \leq k_{m'} \leq 2\pi$ in Eq. (4), for momenta $k_m, k_{m'}$ along the y−direction, with $b_1(l,k)$ the Fourier transform of $b_1(l,j)$. The analysis now is completely analogous to the SLG case [13]. Namely, the boundary condition (2), conveniently rewritten as $\sum_{k_m} b_1(-1, k_m)e^{ik_m j} = -\sum_{k_{m'}}(1+e^{ik_{m'}})b_1(0, k_{m'})e^{ik_{m'}j}$, is satisfied for all k_m and $k_{m'}$ in the ranges indicated above by choosing $b_1(-1, k_m) = 1$ and $b_1(0, k_{m'})(1+e^{ik_{m'}}) = 1$. Going from lattice indices (l,j) to distances (x,y) we obtain exactly the result given by Eq. (1). Therefore, for a vacancy at $A1/B2$ sites in BLG a quasi-localized (decaying as $1/r$) zero-energy mode exists around the vacancy, living in the same layer but opposite sublattice.

Consider now a vacancy at $B1/A2$ sites, sketched in Fig. 2(b). The zigzag- and Klein-edge states with a finite amplitude, respectively, over sites $(-1, j)$ and $(0, j)$ of layer 1, are now those of the bilayer type. These states have amplitudes over layer 1 still given by Eqs. (3) and (4), with the replacement $b \to a$. Additionally, they have also finite amplitudes over layer 2, which can be written as

$$a_2(l < 0, j) = \frac{\gamma_1}{t} \sum_{k_m} a_1(-1, k_m)(l+1) D_{k_m}^{-(l+2)} e^{ik_m(\frac{l+2}{2}+j)}, \quad (5)$$

$$a_2(l \geq 0, j) = \frac{\gamma_1}{t} \sum_{k_{m'}} a_1(0, k)(l+1) D_{k_{m'}}^{-(l+1)} e^{ik_{m'}(\frac{l+1}{2}+j)}, (6)$$

with momenta $k_m, k_{m'}$ restricted to the intervals mentioned before. An important point to note is that the boundary condition reads exactly the same as in Eq. (2), with the replacement $b \to a$. Even though we are using zigzag- and Klein-edge states which have finite amplitudes in both layers, it happens that, by construction, the weight (5) of the zigzag surface state at layer 2 is such that $a_2(-1, j) = 0$, and thus the matching condition at this layer is satisfied by default. At this point the derivation follows closely that for a vacancy at $A1/B2$. Noting that in layer 1 we have to match exactly the same edge-state solutions given by Eqs. (3) and (4), with $b \to a$, and that in layer 2 Eqs. (5) and (6) can also be written in the same form as Eqs. (3) and (4), apart from the term $(l+1)\gamma_1/t$, we arrive at the following zero-mode behavior,

$$\Upsilon(x, y) \sim \Psi(x, y) \left[1, x\, \gamma_1/t\right], \qquad (7)$$

where $\Psi(x, y)$ is the quasi-localized state given in Eq. (1), and the two component wave function refers to the two layers; first and second components for the first and second layers, respectively. This is a delocalized state, with the peculiarity of being quasi-localized in one layer (where the vacancy sits) and delocalized in the other where it goes to a constant when $r \to \infty$.

The analytic construction used for the minimal model in BLG applies directly to MLG and graphite with Bernal stacking along the lines of Ref. [17]. The quasi-localized state (1) is a solution in any multilayer with a $A1/B2$-vacancy. For a $B1/A2$-vacancy the solution is a generalization of state (7) with a quasi-localized component in the layer where the vacancy resides and delocalized components in the layers right on top and below this one: $\Phi(x, y) \sim \Psi(x, y) \left[1, x\, \gamma_1/t, x\, \gamma_1/t\right]$.

The continuum limit.— Both the conventional [Eq. (1)] and the unconventional [Eq. (7)] solutions are fully consistent with the low-energy approximation for BLG [4]. Far from the vacancy the zero modes must obey $\partial_{\bar{z}}^2 \psi_{B1}(z, \bar{z}) = 0$ and $\partial_z^2 \psi_{A2}(z, \bar{z}) = 0$ at $\mathbf{K}$, where $z = x + iy$ and $\bar{z} = x - iy$, and a similar set at $\mathbf{K'}$ with z replaced by $\bar{z}$ everywhere. An obvious solution has $\psi_{B1}(z, \bar{z}) = f(z)$ and $\psi_{A2}(z, \bar{z}) = 0$, or $\psi_{B1}(z, \bar{z}) = 0$ and $\psi_{A2}(z, \bar{z}) = f(\bar{z})$, with $f(z)$ analytic. Adding the contribution of the two K's we see that Eq. (1) is precisely of this form; the amplitude over the sublattice opposite to the vacancy behaving as $1/z + 1/\bar{z}$, analogous to the quasi-localized solution in SLG [13]. Interestingly, the bilayer model also supports solutions with $\psi_{B1}(z, \bar{z}) = \bar{z}f(z)$ and $\psi_{A2}(z, \bar{z}) = 0$, or $\psi_{B1}(z, \bar{z}) = 0$ and $\psi_{A2}(z, \bar{z}) = zf(\bar{z})$. Equation (7) at the low-energy sublattice opposite to the vacancy is indeed a combination of the stated solutions, namely $\bar{z}/z + z/\bar{z}$ [18].

Vacancies in the gapless case.—The analytic results just presented are for $\gamma_3 = 0$. A finite γ_3 is crucial for the existence of the quasi-localized state (1); otherwise a finite density of delocalized states exists in the same energy region [see Fig. 1(b)-(c)]. This is addressed numeri-
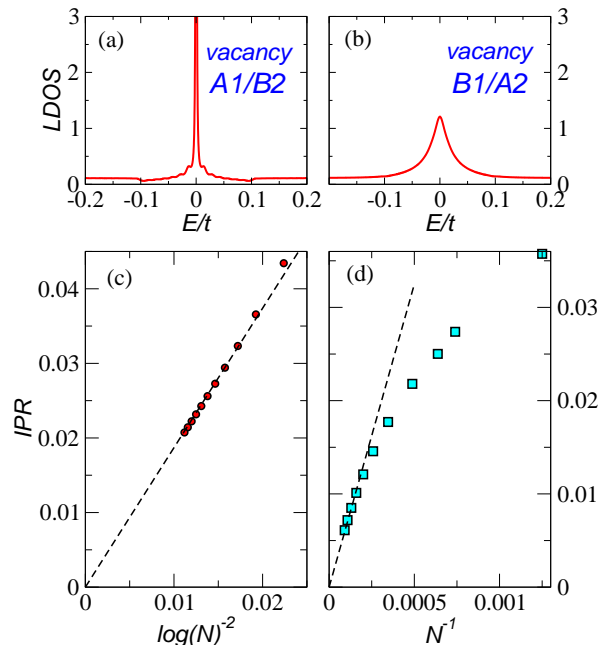

Figure 3: (color online). LDOS (a)-(b) and IPR (c)-(d) for a vacancy at sublattice $A1/B2$ (left panels) and $B1/A2$ (right panels). The LDOS is computed at a lattice site closest to the vacancy. The IPR is for the zero-energy mode induced by the vacancy. Lines are guides to the eyes.

cally in the following. We also show that the delocalized character of the new solution (7) persists in the presence of a finite γ_3. The localization character of vacancy-induced modes is studied through finite-size-scaling of the inverse participation ratio (IPR). The later is defined as $\mathcal{P}_\nu = \sum_i^N |\varphi_\nu(i)|^4$ for the eigenstate ν, where $\varphi_\nu(i)$ is its amplitude at site i. We perform exact diagonalization on small clusters with N up to 2×100^2 sites. The IPR for *extended*, *quasi-localized*, and truly *localized* states scales distinctively with N [16]. While for extended states we have $\mathcal{P}_\nu \sim N^{-1}$, for quasi-localized states the $1/r$ decay implies $\mathcal{P}_\nu \sim \log(N)^{-2}$ (consequence of the definition of the IPR in terms of normalized eigenstates). For localized wavefunctions the significant contribution to $\mathcal{P}_\nu$ comes from the sites in which they lie, and a size independent $\mathcal{P}_\nu$ shows up. Additionally to the IPR, we analyze the changes induced in the LDOS for sites around the vacancy. The LDOS is computed using the recursive Green's function method in clusters with $N = 2 \times 1400^2$, from which the thermodynamic limit can be inferred.

In Fig. 3(a) and 3(b) we show the LDOS at a lattice site closest to a vacancy located in sublattice $A1/B2$ and $B1/A2$, respectively. The sharp resonance at zero energy in the former case is in agreement with the presence of a quasi-localized state, while the broader feature in the later may be attributed to the delocalized wavefunction induced by a vacancy in $B1/A2$, which still presents a quasi-localized component in the layer where the va-
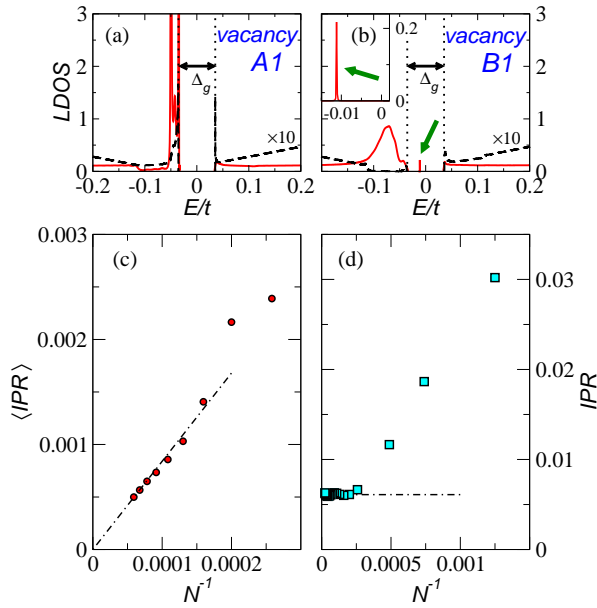
Figure 4: (color online). LDOS for a vacancy at sublattice $A1$ (a) and $B1$ (b) for a finite gap, $V = 0.1t$. The LDOS is computed at a lattice site closest to the vacancy. Dashed lines are for the perfect lattice. (c) IPR averaged over the gap-edge resonance shown in (a). (d) IPR for the in-gap mode shown in (b). Dashed-dotted lines are guides to the eyes.

cancy sits (and thus the feature). This interpretation is fully corroborated by the IPR scaling analysis shown in Fig. 3(c) and 3(d) for a vacancy in $A1/B2$ and $B1/A2$, respectively: quasi-localized state in the former case, and delocalized in the later.

Vacancies in the gaped case.—When a finite electric field E_z is present, a gap $\Delta_g = [V^2\gamma_1^2/(V^2+\gamma_1^2)]^{1/2}$ opens between conduction and valence bands [5]. The quasi-localized state due to a vacancy at sublattice $A1/B2$ becomes a resonance around $\pm V/2$ in the gaped case, as seen in the LDOS shown in Fig. 4(a) for a site closest to the vacancy. A strong resonance is seen around $-V/2$ for a vacancy at $A1$ (we used $V = 0.1t$), apart from the known gap edge divergence at $-\Delta_g/2$ characteristic of the perfect lattice (dashed line) [19]. A vacancy at $B2$ gives identical results with $E \to -E$. Such a vacancy-induced state living in the continuum is expected to be delocalized. This is confirmed by the IPR scaling as N^{-1} [20], as shown in Fig. 4(c).

For a vacancy at sublattice $B1/A2$, which originates the atypical delocalized state discussed above when no gap is present, a truly localized state inside the gap is induced when $E_z \neq 0$. This is suggested by the sharp feature seen inside the gap in the LDOS for a site closest to the vacancy, as shown in Fig. 4(b) and zoomed in the inset (marked by arrows). The IPR scaling to a constant, as seen in Fig. 4(d), fully confirms the localized nature of this vacancy-induced state. Its asymmetric weight over the two layers explains why it appears off zero-energy:

being negative for a $B1$ vacancy (layer 1 at an electro-static energy $-V/2$), as shown in Fig. 4(b), and positive, symmetrically placed with respect to the center of the gap, for a $A2$ vacancy (layer 2 at an electrostatic energy $+V/2$).

Conclusions.—We have found a new type of zero mode state in BLG with special features: in the absence of a gap it is quasi-localized in one of the layers and delocalized in the other and in the presence of a gap becomes fully localized inside the gap. The results obtained in this work are directly applicable to MLG and graphite with Bernal stacking. The findings here reported can be important to understand recent experiments done in thin films of graphite irradiated with protons whose main effect is to produce single vacancies on the sample [21]. These samples show an enhanced local ferromagnetism that can be due to the local moments associated to the zero modes described in this work, and also a better conductivity than the untreated samples with less defects pointing to the idea that the delocalized states induced by the vacancies contribute to the conductivity. An enhanced conductivity has also been found in acid-treated few-layer graphene [22]. The localized state found in the gaped case can also provide a natural explanation for the observation of localization inside the gap in the biased BLG [7] and is in agreement with previous results obtained with impurity models in the continuum [23].

[1] K. Novoselov *et al.*, Science **306**, 666 (2004).
[2] L. A. Ponomarenko *et al.*, Science **320**, 356 (2008).
[3] A. H. Castro Neto *et al.*, Rev. Mod. Phys. **81**, 109 (2009).
[4] E. McCann and V. I. Fal'ko, Phys. Rev. Lett. **96**, 086805 (2006).
[5] E. McCann, Phys. Rev. B **74**, 161403(R) (2006).
[6] E. V. Castro *et al.*, Phys. Rev. Lett. **99**, 216802 (2007).
[7] J. B. Oostinga *et al.*, Nat. Mater. **7**, 151 (2008).
[8] K. I. Bolotin *et al.*, Solid State Commun. **146**, 351 (2008).
[9] X. Du *et al.*, Nature Nanotech. **3**, 491 (2008).
[10] M. Monteverde *et al.*, arXiv:0903.3285v2.
[11] M. H. Gass *et al.*, Nature Nanotech. **3**, 676 (2008).
[12] S. Choi *et al.*, J. Phys.: Condens. Matter **20**, 235220 (2008).
[13] V. M. Pereira *et al.*, Phys. Rev. Lett. **96**, 036801 (2006).
[14] E. V. Castro *et al.*, Phys. Rev. Lett. **100**, 026802 (2008).
[15] Its analytic form is easily obtained by inverting the 2×2 matrix appearing in equation (4) of reference [14], and following the steps outlined there.
[16] V. M. Pereira, J. M. B. Lopes dos Santos, and A. H. Castro Neto, Phys. Rev. B **77**, 115109 (2008).
[17] E. V. Castro, N. M. R. Peres, and J. M. B. L. dos Santos,

Europhys. Lett. **84**, 17001 (2008).

[18] Equation (7) is a linear combination of $e^{i\mathbf{K}\cdot\mathbf{r}}\bar{z}/z$ at K and $e^{i\mathbf{K'}\cdot\mathbf{r}}z/\bar{z}$ at K' with the plane waves $e^{i\mathbf{K}\cdot\mathbf{r}}$ and $e^{i\mathbf{K'}\cdot\mathbf{r}}$ – the two later reflecting the particular zigzag line used to match zigzag and Klein edge states.

[19] F. Guinea, A. H. Castro Neto, and N. M. R. Peres, Phys. Rev. B **73**, 245426 (2006).

[20] As usually done in regions of continuum DOS, the IPR is an average over states in an energy bin $\Delta E = 0.2t$ around the resonance.

[21] A. Arndt *et al.*, arXiv:0905.2945v1 [cond-mat.mtrl-sci].

[22] S. H. M. Jafri *et al.*, arXiv:0905.1346v1 [cond-mat.mtrl-sci].

[23] J. Nilsson and A. H. Castro Neto, Phys. Rev. Lett. **98**, 126801 (2007).